The Meteoritical Society

Meteoritics & Planetary Science 1–17 (2024)
doi: 10.1111/maps.14134

How many Vesta-like bodies existed in the asteroid belt?

T. H. BURBINE [1,2]*, R. C. GREENWOOD [3], B. ZHANG [4], and P. C. BUCHANAN [5]

[1]Department of Astronomy, Mount Holyoke College, South Hadley, Massachusetts, USA
[2]Planetary Science Institute, Tucson, Arizona, USA
[3]The Open University, Milton Keynes, UK
[4]Department of Earth, Planetary, and Space Sciences, University of California, Los Angeles, Los Angeles, California, USA
[5]Department of Geology, Kilgore College, Kilgore, Texas, USA
***Correspondence**
T. H. Burbine, Department of Astronomy, Mount Holyoke College, 50 College Street, South Hadley, MA 01075, USA.
Email: tburbine@mtholyoke.edu

(Received 16 March 2023; revision accepted 01 January 2024)

Abstract–Asteroid 4 Vesta is typically thought to be the parent body of the HED (howardite, eucrite, and diogenite) meteorites due to spectral similarities. The discovery of asteroids far from Vesta with HED-like spectra like (1459) Magnya and HED-like meteorites (e.g., NWA 011) with anomalous oxygen isotopic values compared to typical HEDs is evidence that other Vesta-like bodies formed. We broadly define a Vesta-like body as a differentiated object with a crust composed primarily of low-Ca pyroxene and plagioclase feldspar. We estimate the number of Vesta-like bodies that did form by looking at the astronomical evidence; the oxygen isotopic, chemical, and petrologic evidence; and the iron meteorite evidence. Assuming that fragments of Vesta were scattered from Vesta by giant planet migration, we conservatively estimate that at least two Vesta-like bodies (Vesta and the Magnya parent bodies) existed. From the oxygen isotopic, chemical, and petrologic evidence, we also conservatively estimate that seven Vesta-like bodies formed. Analyses of iron meteorites indicate that there may be as many as 23 Vesta-like bodies (Vesta, 10 magmatic iron groups, South Byron trio, Emsland/Mbosi duo, 10 ungrouped irons). This estimate from iron meteorites is most certainly an overestimation due to the existence of a number of non-HED crustal/mantle fragments that potentially originated from bodies with magmatic iron cores. Using our three estimates as a guide, we predict that there were ~10 Vesta-like bodies (including Vesta) that formed in the early solar system. Only Vesta remains intact with the others being disrupted early in solar system history.

INTRODUCTION

Asteroid 4 Vesta has long been known to have a distinctive reflectance spectrum (Figure 1) very similar to the spectra of the pyroxene-rich basaltic HED (howardite, eucrite, and diogenite) meteorites (e.g., Larson & Fink, 1975; McCord et al., 1970). Vesta (Figure 2) is the second largest body in the asteroid belt with a diameter of ~525 km. Spectral and geochemical analyses by the Dawn spacecraft (e.g., McSween et al., 2014; Russell et al., 2012) are also consistent with HED-like surface for Vesta.

Many smaller bodies in and near the Vesta family were also found to have HED-like spectra (Binzel & Xu, 1993). These objects with HED-like spectra are generally referred to as V-types. Binzel and Xu (1993) did classify some bodies with visible spectra similar to those observed in diogenites as J-types for the Johnstown diogenite; however, the J-type classification is currently not used and these objects are given V-type designations. V-type objects have very distinctive absorption features due to low-Ca pyroxene (Figure 1). Low-Ca pyroxene spectra tend to have two strong absorption bands centered at ~0.9 (Band I) and ~1.9 μm (Band II). However, near-

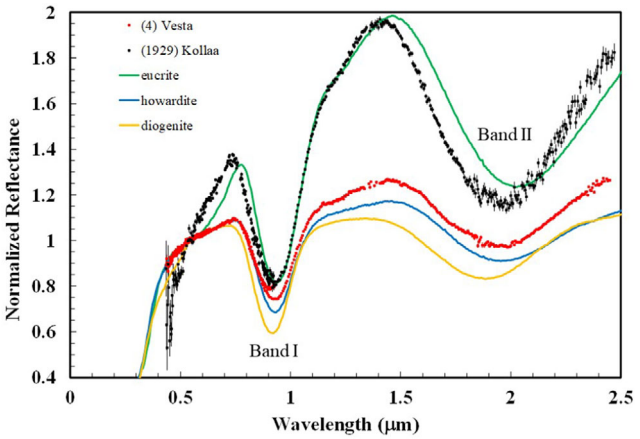

FIGURE 1. Normalized reflectance spectra of 4 Vesta (filled red squares), (1929) Kollaa (filled black squares), the monomict eucrite Bouvante (green line), howardite Elephant Moraine (EET) 87503 (blue line), and diogenite Johnstown (orange line). The visible asteroid spectra of Vesta and Kollaa are from Bus and Binzel (2002a, 2003). The IRTF (Infrared Telescope Facility) spectrum of Vesta is from Reddy and Sanchez (2016) and the IRTF spectrum of Kollaa is from Bus (2011). The visible and near-infrared spectra for each asteroid are spliced together. The Bouvante spectrum is from Burbine et al. (2001), the EET 87503 spectrum is from Hiroi et al. (1994), and the Johnstown spectrum is from Hiroi et al. (1995). All of the meteorite reflectance spectra were acquired at RELAB and are normalized to unity at 0.55 μm. The particle sizes of the meteorites are less than 25 μm. The uncertainties for the asteroid reflectance spectra are one-sigma. The uncertainties for the meteorite reflectance spectra are not plotted since they are extremely small. Band I is at ~0.9 μm and Band II is at ~1.9 μm.

infrared spectral observations are much more conclusive since both pyroxene bands can be characterized. V-types that can be potentially linked to Vesta are typically called vestoids. V-type bodies can be identified through both visible and/or near-infrared observations.

It is now generally accepted that Vesta is the parent body of HEDs due to its spectral similarity, large size, and the presence of vestoids between Vesta and meteorite-supplying resonances. However, Lazzaro et al. (2000) identified a body (1459) Magnya, with an HED-like near-infrared spectrum out to ~1.65 μm in the outer part of the asteroid belt (3.15 au), far from Vesta (2.36 au). The HED-like characteristics of Magnya were confirmed by Hardersen et al. (2004) using a longer wavelength coverage (Figure 3). Subsequently, a meteorite originally classified as a eucrite, Northwest Africa (NWA) 011, due to its texture and bulk mineralogy was found to have oxygen (O) isotopic composition values very different from typical HEDs (Yamaguchi et al., 2002). Subsequently, more V-types have been observed in the outer belt (e.g., Licandro et al., 2017) and more HEDs with anomalous oxygen isotopic values (e.g., Bunburra Rockhole) compared to typical HEDs have been identified (e.g., Benedix et al., 2017; Greenwood et al., 2017; Mittlefehldt et al., 2022; Scott et al., 2009; Wiechert et al., 2004).

In this work, we will discuss the evidence for other Vesta-like bodies in the asteroid belt, in addition to Vesta itself. We first discuss what we define as a Vesta-like body. We then look at the astronomical evidence for V-types not related to Vesta. We also review the relevant isotopic, chemical, and petrologic analyses of HEDs; and implications from iron meteorites. Our overall objective was to estimate how many Vesta-like bodies originally existed and gain an insight into how widespread were the processes that led to the formation of differentiated crusts in the asteroid belt.

VESTA-LIKE BODIES

We broadly define a Vesta-like body as a differentiated asteroid-sized object with a crust composed predominantly of low-Ca pyroxene and plagioclase feldspar. HEDs contain varying amounts of these two components. During differentiation, denser materials, such as Fe-Ni metal and sulfides, tend to sink to the core, while lighter materials tend to rise to the surface. Eucrites are primarily composed of a variety of pyroxenes and anorthite-rich plagioclase, while diogenites are primarily composed of magnesian-rich low-Ca pyroxenes (Mittlefehldt et al., 1998). Howardites are polymict breccias that contain both eucritic and diogenitic fragments. Eucrites have been subdivided into a number of subtypes based on compositional or petrographic criteria due to the large variety of igneous processes and impact events occurring on their parent body.

Differentiation of early solar system bodies was most likely caused by the decay of ^{26}Al, which produces significant amounts of heat and whose decay products have been identified by isotopic analysis of plagioclase in some eucrites (e.g., Piplia Kalan; Srinivasan et al., 1999). We want to emphasize that the differentiation and the formation of an Fe-Ni core does not always result in an HED-like crust. Jurewicz et al. (1991, 1993) found that partial melts of carbonaceous chondritic material could resemble eucrites at low oxygen fugacities and angrites at high oxygen fugacities. Angrites have extremely oxidized compositions relative to eucrites. Andesitic crusts also formed in the asteroid belt (Day et al., 2009; Nicklas et al., 2022; Srinivasan et al., 2018). Andesites are more silica-rich than basaltic rocks. Also present among meteorites are aubrites, which are enstatite-rich igneous fragments (e.g., Watters & Prinz, 1979) from the crusts or mantles of extremely reduced differentiated bodies. Potential meteoritical crustal material such as angrites and aubrites have very different spectral properties in the

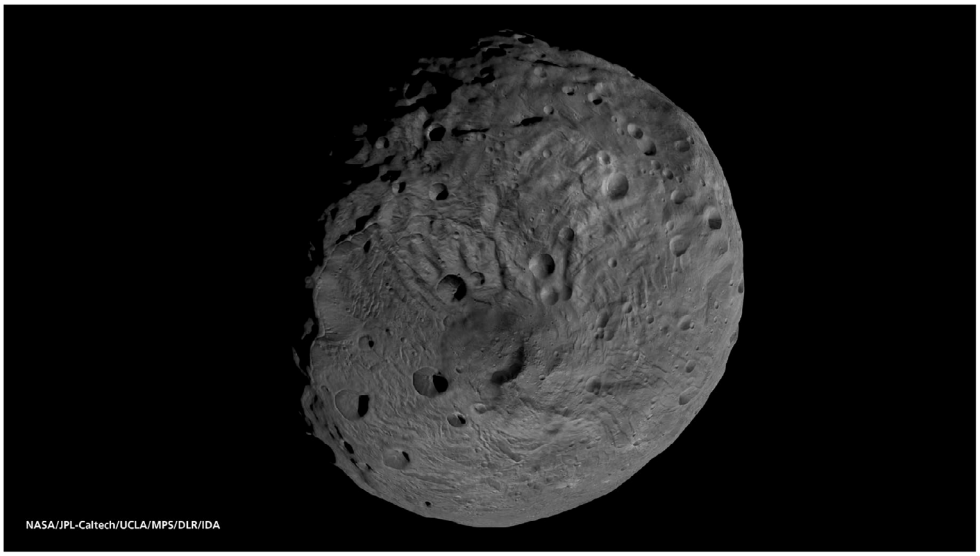

FIGURE 2. Image taken by Dawn's Framing Camera of Vesta's south pole. The Rheasilvia basin overlays the Veneneia basin. Image credit: NASA/JPL-Caltech/UCLA/MPS/DLR/IDA.

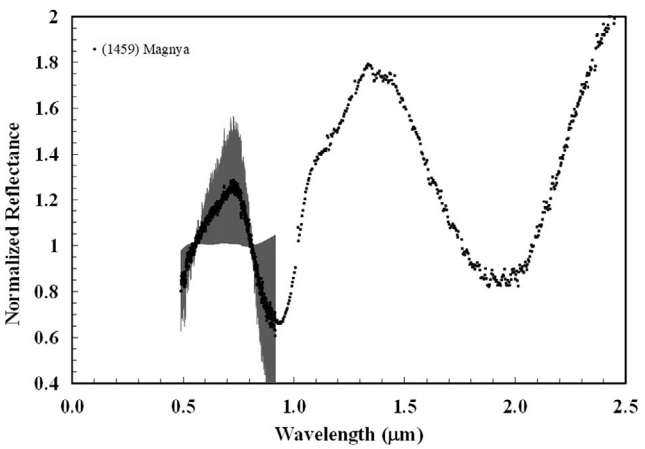

FIGURE 3. Normalized reflectance spectra of (1459) Magnya (filled black squares). The visible asteroid spectrum of Magnya is from Lazzaro et al. (2006) and the IRTF spectrum is from Hardersen et al. (2004). The uncertainties for the Lazzaro et al. (2006) spectrum are one-sigma while the Hardersen et al. (2004) spectrum does not have published uncertainties (Hardersen, 2016).

visible and near-infrared (Burbine et al., 2002, 2006) than HEDs.

ASTRONOMICAL EVIDENCE

Most V-types are identified through visible spectral (Alvarez-Candal et al., 2006; Binzel & Xu, 1993; Bus & Binzel, 2002a, 2002b; Hicks et al., 2014; Lazzaro et al., 2004; Xu et al., 1995) or color surveys in the visible (Carvano et al., 2010; Oszkiewicz et al., 2023; Roig & Gil-Hutton, 2006) or near-infrared range (Colazo et al., 2022; Licandro et al., 2017; Mansour et al., 2020). Near-infrared spectral surveys (e.g., DeMeo et al., 2009; Duffard et al., 2004; Hardersen et al., 2014, 2015, 2018; Moskovitz et al., 2010) have been used to "confirm" the HED-like nature of these objects.

We do assume that most V-types have HED-like mineralogies. Most HED spectra classify as V-types using the Bus–DeMeo taxonomy (Burbine et al., 2019; Khanani et al., 2021). Matlovič et al. (2020) found a success rate of over 85% in confirming V-type classifications using near-infrared spectra from the MOVIS (Moving Objects from VISTA Survey) catalog but that most of the misclassifications occurred among objects located past the 3:1 resonance. Silicates from acapulcoites/lodranites (primitive achondrites) can have spectral properties similar to HEDs (e.g., Lucas et al., 2019) and these silicates could potentially classify as V-types. However, acapulcoites/lodranites tend to be rich in metallic iron. Since a significant metallic iron component tends to reduce the pyroxene band strengths of acapulcoite/lodranite material, we expect acapulcoite/lodranite mineralogies to be relatively rare among V-types. Modified Gaussian Modeling of some S-types had high-Ca pyroxene to total pyroxene ratios (≥0.4) consistent with basaltic assemblages (Sunshine et al., 2004) so not all HED and HED-like material in the asteroid belt would just be present as V-types.

The source of most vestoids is thought to be the Rheasilvia basin (e.g., Sykes & Vilas, 2001; Thomas et al., 1997), which is located at Vesta's south pole (Figure 2). The Rheasilvia basin has an estimated age of ~0.8–0.9 Ga

ago from the work of Schenk et al. (2022), which is roughly consistent with the estimated formation age of the Vesta family (e.g., Asphaug, 1997; Carruba et al., 2007; Nesvorný et al., 2008). However, Schmedemann et al. (2014) has estimated a much older age of 3.5 Ga for the Rheasilvia basin. The Rheasilvia basin has a diameter of ~500 km and a depth of ~19 km (Schenk et al., 2012).

The identification of the Magnya's HED-like near-infrared spectrum (Lazzaro et al., 2000) demonstrated that basaltic material exists in the outer main belt. However, Michtchenko et al. (2002) found that it was extremely difficult to derive Magnya from Vesta. Magnya tends to be much larger than other V-types (excluding Vesta), with an estimated diameter of 17 km (Delbo et al., 2006). Almost all known V-types have estimated diameters of 10 km or less (e.g., Oszkiewicz et al., 2020). Brasil et al. (2017) argued that Magnya's relatively large size (~17 km) compared to other vestoids, which have estimated diameters less than 10 km, is not consistent with Magnya being a fragment of Vesta. Tens of vestoids with diameters of ~20 km should exist if Magnya was a fragment of Vesta.

Hardersen et al. (2004) confirmed Magnya's spectral similarity to that of HEDs with longer wavelength coverage but interpreted Magnya's spectrum as indicating a pyroxene chemistry that is ~10 mole% ferrosilite (Fs) less than Vesta's pyroxenes. Burbine et al. (2023) interpreted Magnya's mineralogy as being consistent with eucrites.

We plot proper sine of inclination versus proper semi-major axis (au) for V-types classified using visible spectra or visible or near-infrared colors with no corresponding near-infrared spectra (~3700 bodies), V-types with near-infrared spectra (~130), Vesta family members (~15,000), and all asteroids with calculated proper elements (~585,000; Figure 4; Novaković et al., 2022). Vesta and Magnya are plotted separately. We do not plot objects with visible or near-infrared spectra that are not consistent with typical V-type spectra, such as (2579) Spartacus (Angrisani et al., 2023; Moskovitz et al., 2010), (5051) Ralph (Bus & Binzel, 2002a, 2002b), (7302) 1993 CQ (Hardersen et al., 2018; Matlovič et al., 2020), (7472) Kumakiri (Burbine et al., 2011), (10537) 1991 RY_{16} (Moskovitz et al., 2008), (11699) 1998 FL_{105} (Hardersen et al., 2018), (14390) 1990 QP_{10} (Matlovič et al., 2020), (24014) 1999 RB_{118} (Hardersen et al., 2018), and (26417) Michaelgord (Hardersen et al., 2018). The distribution of V-types in the inner main belt is cut by the sloping ν_6 secular resonance (Carruba et al., 2018) at the inner edge of the belt and the 3:1 mean-motion resonance at 2.5 au. Other secular resonances appear to have affected the orbits of a number of other V-types (Carruba et al., 2005). We do not plot objects in strong secular resonances due to the difficulty in calculating "accurate" proper elements for these objects.

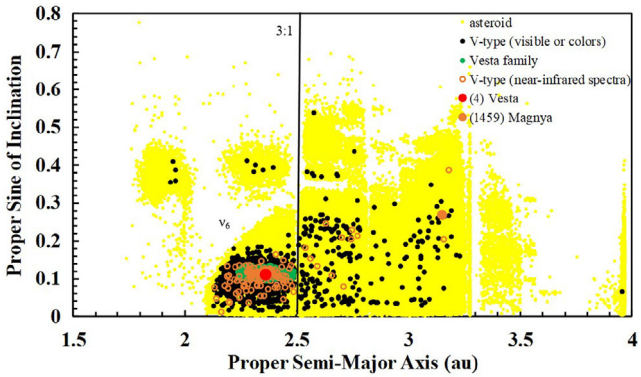

FIGURE 4. Plot of proper sine of inclination versus proper semi-major axis (au) for all asteroids (yellow dots; Novaković et al., 2022), V-types (black dots) that have been identified by various visible spectra surveys or visible or near-infrared color surveys with no near-infrared spectral data, Vesta family members (green dots) (Nesvorny, 2015), Vesta (red filled circle), V-types that have near-infrared spectra consistent with an HED-like mineralogy (orange open circles), and Magnya (orange filled circle). Our V-types include objects with HED-like visible spectra or colors that have been classified as either V-types, J-types, or V_p-types. The plotted Vesta family members have been identified just by dynamical criteria since most of the ~15,000 family members have not been classified since they have not been observed as part of spectral or color surveys. The ν_6 secular resonance at the inner edge of the belt and the 3:1 mean-motion resonance are also identified.

In Figure 4, the distribution of V-types in the inner main belt can be seen to be much more spread out than can be accounted for just by recognized members of the Vesta family. This large spread could be due to a number of factors such as large ejection velocities from Vesta, Yarkovsky drift, and/or gravitational interactions with Vesta (e.g., Carruba et al., 2007). Fragments of Vesta also appear to have passed through the 3:1 mean-motion resonance to larger semi-major axes. Roig et al. (2008) calculated that a ~5-km-diameter vestoid would have an ~1% probability of crossing the 3:1 resonance due to the Yarkovsky effect. Larger bodies would have a lower probability of crossing the resonance due to the Yarkovsky effect having less of an effect for bigger objects. However, modeling by Brasil et al. (2017) found that giant planet migration early in solar system history could affect the orbits of fragments of Vesta and produce the current distribution of Sloan Digital Sky Survey (SDSS) and MOVIS V-types except for Magnya. These V-types located past the 3:1 resonance could have been produced by an impact that predated by billions of years the impact that produced the current Vesta family. The Veneneia basin was estimated to have a formation age lower limit of ~3.7 Ga (Schmedemann et al., 2014) and its formation

could have produced some of the V-types that are located far from Vesta.

As seen in Figure 4, most V-types located past the 3:1 resonance have not been spectrally observed in the near-infrared and, therefore, have not had their HED-like nature confirmed. There are also some high-inclination V-types in the inner belt that also have not been spectrally observed in the near-infrared. Many of these high-inclination V-types are in the Hungaria region, which have semi-major axes between ~1.78 and ~2.06 au (Correa-Otto & Cañada-Assandri, 2018). There is also a V-type located at ~4 au, which has also not been spectrally observed in the near-infrared.

Other sources for middle and outer belt V-types have also been proposed. Carruba et al. (2014) looked at the distribution of V-types past the 3:1 resonance and proposed that these bodies dynamically evolved from the Eunomia and Merxia/Agnia families on a time scale of ~2 Ga. Huaman et al. (2014) identified three asteroidal sources that could explain the distribution of V-types located far from Vesta.

A conservative estimate for the number of Vesta-like bodies from the astronomical evidence would be two: Vesta and the Magnya parent body. However, many more Vesta-like bodies most certainly existed if these large bodies were disrupted very early in solar system history and only a relatively few fragments from each of these objects are observable today. The evidence for any Vesta-like bodies disrupted in the inner belt would probably be obscured by V-types resulting from the impact that caused the Vesta family.

ISOTOPIC, CHEMICAL, AND PETROLOGIC EVIDENCE

Over 2800 HED meteorites have currently been identified on Earth (Meteoritical Bulletin Database, 2024). Several pieces of evidence suggest that more than one early solar system body experienced Vesta-like melting and differentiation. Specifically, oxygen isotopic analyses indicate that more than one other Vesta-like body existed (Greenwood et al., 2020; Mittlefehldt et al., 2022; Scott et al., 2009). Almost all HEDs have chromium (Cr) and titanium (Ti) isotopic compositions consistent with most other differentiated meteorites plus ordinary and enstatite chondrites (Kleine et al., 2020; Warren, 2011). Meteorites with these Cr and Ti isotopic compositions are called non-carbonaceous (NC) meteorites and plot distinctly away from the region defined by Cr and Ti isotopic values for carbonaceous chondrite (CC) meteorites. The identification of isotopic differences between NC and CC meteorites indicates that at least two reservoirs of material existed in the solar system. NC meteorites are generally believed to have formed in the inner part of the solar system, whereas CC meteorites are thought to have formed in the outer solar system (e.g., Warren, 2011).

An example of a CC achondrite is NWA 011. Yamaguchi et al. (2002) described NWA 011 as a eucrite in terms of texture and bulk mineralogy. However, NWA 011 had a distinctly different oxygen isotopic composition than typical HEDs ($\Delta^{17}O$ = 0.24‰). NWA 011 has a $\Delta^{17}O$ of −1.6‰ (Floss et al., 2005; Yamaguchi et al., 2002). NWA 011 also has Cr and Ti isotopic compositions consistent with CC meteorites, indicating that NWA 011 formed in the outer solar system (Warren, 2011). A large number of meteorites appear paired with NWA 011, including NWA 2400, NWA 2976, NWA 4587, and NWA 4901 (Meteoritical Bulletin Database, 2024). NWA 011 has also been linked to Magnya (Floss et al., 2005) due to Magnya's location in the outer asteroid belt and apparent derivation from a basaltic body that is not Vesta. The existence of NWA 011 indicates that Vesta-like bodies formed in both the NC and CC regions of the solar system.

Another group of achondrites have been found to have low-Ca pyroxene-rich compositions but anomalous $\Delta^{17}O$ values (−1.1‰) and Cr and Ti isotopic compositions consistent with CC meteorites. These meteorites include NWA 6693 (Warren et al., 2013), NWA 6704 (Hibiya et al., 2019), NWA 6926 (Ruzicka et al., 2014), and NWA 10132 (Sanborn et al., 2018). NWA 6704 was found by McGraw et al. (2020) to have a visible and near-infrared reflectance spectrum that would classify it as a V-type. However, NWA 6693 (Warren et al., 2013) and NWA 6704 (Hibiya et al., 2019) have siderophile (iron-loving) element abundances that are nearly chondritic, which implies that their parent bodies did not undergo differentiation.

Another well-studied anomalous HED is Bunburra Rockhole (e.g., Benedix et al., 2017; Spivak-Birndorf et al., 2015; Spurný et al., 2012). Bunburra Rockhole was observed to fall in Australia by the Desert Fireball Network and approximately 300 g was recovered (Spurný et al., 2012). This meteorite's calculated orbit indicates that it most likely originated from the innermost main belt by the ν_6 secular resonance (Spurný et al., 2012). Bunburra Rockhole has a mineralogy and petrology similar to noncumulate eucrites (Spivak-Birndorf et al., 2015). Bunburra Rockhole's mean $\Delta^{17}O$ of −0.134‰ is distinctly different from HEDs (Benedix et al., 2017). Bunburra Rockhole has a Cr isotopic composition consistent with being a NC meteorite but its $\varepsilon^{54}Cr$ value is different than most HEDs (Benedix et al., 2017).

Meteorites from different planetary bodies tend to define distinct trend lines (slope ~0.5) on a three-oxygen

isotope diagram (e.g., Clayton, 2003; Greenwood et al., 2020). This characteristic likely reflects the fact that these bodies underwent early extensive melting and isotopic homogenization (Greenwood et al., 2005, 2006). The basaltic and cumulate eucrites and the diogenites define a relatively uniform O-isotope trend line (Figure 5), consistent with being derived from a parent body that underwent this type of melting and isotopic homogenization (Greenwood et al., 2005). Cumulate eucrites are distinguished from basaltic eucrites by trace element patterns or petrologic features indicative of crystal accumulation (e.g., Mittlefehldt & Lindstrom, 1993). We call these typical HEDs. Thus, samples that have O-isotope compositions that deviate from the typical HED trend line may be derived from parent bodies other than Vesta. We call these anomalous HEDs. The incorporation of carbonaceous chondritic precursors or impactors will tend to decrease (move down in the plot) the calculated $\Delta^{17}O$ of an HED while the incorporation of ordinary chondritic precursors or impactors will tend to increase (move up in the plot) the calculated $\Delta^{17}O$ of an HED.

As discussed by Mittlefehldt et al. (2022), there is a certain level of circular reasoning about how isotopically "normal" and "anomalous" HED meteorites are defined. Wiechert et al. (2004) argued that isotopic outliers such as Pasamonte indicated that the HED parent body may be isotopically heterogeneous. However, one argument against this possibility is the fact that anomalous samples do not show a symmetrical distribution about the HED mean value. Most identified isotopically anomalous HEDs plot between the EFL (eucrite fractionation line) and angrite fractionation line (AFL) (Figure 5). This variation is not a consequence of terrestrial weathering as Emmaville and Pasamonte are falls and most of the anomalous finds have been chemically treated to remove weathering products, without any evidence for significant isotopic shifts that might reflect incorporation of a terrestrial component (Greenwood et al., 2017; Mittlefehldt et al., 2022; Scott et al., 2009). In addition, there is clear petrologic and geochemical evidence that the HED parent body underwent extensive melting, leading to the development of a magma ocean (e.g., Mandler & Elkins-Tanton, 2013; Righter & Drake, 1997; Ruzicka et al., 1997). Under these conditions, it is likely that complete oxygen isotope homogenization of the HED parent body would have taken place (Greenwood et al., 2005).

The Fe/Mn molar ratio in pyroxenes is known to vary for basalts from different planetary bodies such as the Earth, the Moon, Mars, and typical HEDs (Papike et al., 2003). NWA 011 is known to have a significantly higher Fe/Mn ratio than typical eucrites (Floss et al., 2005; Yamaguchi et al., 2002). Mittlefehldt et al. (2022) found that some eucrites such as brecciated eucrite EET 87542

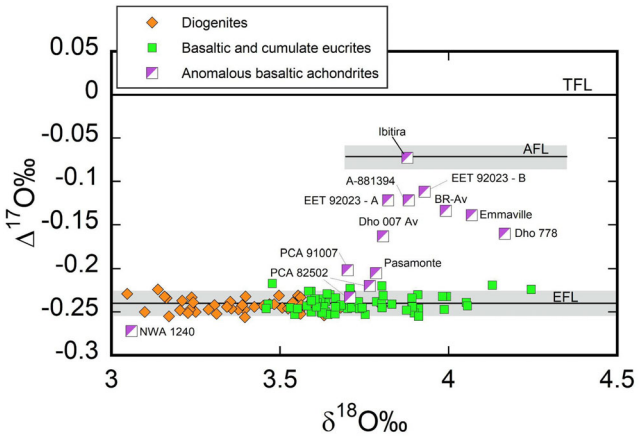

FIGURE 5. Plot of $\Delta^{17}O$ versus $\delta^{18}O$ for diogenites (orange diamonds), basaltic and cumulate eucrites (green squares), and anomalous basaltic achondrites (purple and white squares). *TFL* is the terrestrial fractionation line, *AFL* is the angrite fractionation line, and *EFL* is the eucrite fractionation line. The gray lines are two-sigma uncertainties for the *AFL* and *EFL*. $\Delta^{17}O$ is effectively a measure of the isotopic "distance" from the TFL and is determined using the linearized format of Miller (2002). Data are from Greenwood et al. (2017) and Mittlefehldt et al. (2022). *BR-av* is an abbreviation for the average oxygen isotopic composition for Bunburra Rockhole. Two fractions (A and B) of EET 92023 were measured. NWA 011 and related meteorites ($\Delta^{17}O$ of −1.6‰; Floss et al., 2005; Russell et al., 2005; Yamaguchi et al., 2002) fall far from this region of the oxygen isotope diagram and, therefore, is not plotted. NWA 11916 ($\Delta^{17}O$ of −0.44‰) (Meteoritical Bulletin Database, 2024) is also not plotted since it also falls below the HEDs. Dhofar (Dho) 778 is the only identified anomalous diogenite. NWA 1240 is an impact melt (Barrat et al., 2003). The impact may be causing NWA 1240 to fall below the EFL if some impactor material had been incorporated into it (Mittlefehldt et al., 2022).

and unbrecciated eucrite Queen Alexandra Range (QUE) 94484 with typical oxygen isotopic values had low-Ca pyroxenes with anomalously low values of Fe/Mn compared to typical eucrites. Mittlefehldt et al. (2022) argue that the low Fe/Mn ratio for these meteorites was due to solid-state reduction by sulfur and that these meteorites could have originated on the HED parent body. Mittlefehldt et al. (2022) also found that some eucrites with anomalous oxygen isotopic values had low-Ca pyroxenes with typical eucritic Fe/Mn values. The anomalous monomict eucrite Ibitira (Mittlefehldt, 2005) is known to have a low-Ca pyroxene Fe/Mn ratio distinctly different than typical HEDs while anomalous eucrite Bunburra Rockhole (Benedix et al., 2017) has a low-Ca pyroxene Fe/Mn ratio consistent with typical HEDs.

These anomalous HEDs (Figure 5) have a wide variety of compositional, petrologic, and isotopic characteristics. Only NWA 11916, which is pigeonite-rich (Meteoritical Bulletin Database, 2024), has not been

widely studied. Ibitira is vesicle-rich, which is an extremely rare characteristic in meteorites (e.g., McCoy et al., 2005). The unbrecciated eucrite Pecora Escarpment (PCA) 82502 and the brecciated eucrite PCA 91007, which are paired, are two vesicle-rich eucrites that have slightly anomalous to normal oxygen isotopic values but typical low-Ca pyroxene Fe/Mn ratios. Polymict eucrite Pasamonte is isotopically similar to PCA 82502 and PCA 9100 but petrologically distinct (Mittlefehldt et al., 2017). Basaltic eucrite Emmaville is petrologically similar to other basaltic eucrites but has oxygen isotopic values similar to Bunburra Rockhole, Asuka (A-) 881394, and EET 92023 (Barrett et al., 2017).

A-881394, Bunburra Rockhole, Ibitira, Pasamonte, and PCA 91007 have Cr isotopic compositions offset from typical HEDs (Wimpenny et al., 2019) while EET 92023 has values that are not offset. Within two-sigma error bars, the chromium isotopic compositions for A-881394 and EET 92023 do overlap so derivation from the same parent body for these two meteorites appears reasonable. Benedix et al. (2017) argued that the differences in texture and plagioclase compositions for A-881394 and Bunburra Rockhole imply that these two meteorites come from different parent bodies; however, Wimpenny et al. (2019) argue that the two meteorites could originate from two different magmatic systems on the same parent body due to similarities in $\Delta^{17}O$ and $\varepsilon^{54}Cr$ values. A-881394 has an extremely old Pb-Pb age (4.565 Ga) (Wimpenny et al., 2019), whereas the Pb-Pb age of Bunburra Rockhole appears to have been reset by an impact (Spivak-Birndorf et al., 2015).

Mesosiderites are a mixture of basaltic material and Fe-Ni metal. Silicates from mesosiderites have oxygen isotopic values consistent with typical HEDs. This mixture of crustal and core material is thought to have formed from the impact of an iron core into the basaltic crust of an asteroid with intimate mixing of the two lithologies. However, the pyroxenes in mesosiderites tend to have a wide variation in the Fe/Mn ratio but a relatively small range in the Fe/Mg ratio, whereas HEDs tend to have a wide variation in the Fe/Mg ratio and a relatively small range in the Fe/Mn ratio (LeLarge et al., 2022; Mittlefehldt, 1990). These chemical differences may imply a separate parent body for mesosiderites than Vesta (LeLarge et al., 2022), but this is by no means certain (Haba et al., 2019). However, whether one or two bodies are required for the HEDs and mesosiderites, their closely similar oxygen isotope compositions imply that these lithologies come from asteroids that formed in close proximity to each other in the solar nebula. Cumulate eucrite Dho 007 has been potentially linked to mesosiderites due to experiencing a two-stage thermal history and an enrichment in siderophile elements (Yamaguchi et al., 2006) even though mesosiderites have distinctly different oxygen isotopic compositions (Greenwood et al., 2006; LeLarge et al., 2022). The diogenite Dho 778 has oxygen and chromium isotopic compositions similar to Dho 007 but contains ~44% olivine by volume (Pang et al., 2020).

Using previously published HED oxygen isotopic data, Zhang et al. (2019) estimated that HEDs with anomalous oxygen isotopic values originated from at least five different parent bodies. Scott et al. (2009) argued that NWA 1240, Pasamonte/PCA 91007, A-881394, Ibitira, NWA 011/2400/2976/4587, and NWA 4901 originated from five distinct parent bodies. Greenwood et al. (2020) estimated that basaltic meteorites with a non-HED O-isotope composition may be derived from between five and 11 parent bodies.

Looking at the available oxygen isotopic data, we estimate (Table 1) that there is evidence for seven Vesta-like bodies, which includes the HED-parent body. Greenwood et al. (2020) also proposed seven Vesta-like bodies. We do not include NWA 1240 since it is an impact melt and may have had its oxygen isotopic composition affected by the impactor. As discussed by Mittlefehldt et al. (2022), not all HEDs with anomalous oxygen isotopic data also have anomalous Fe/Mn ratios, which makes it difficult to use the Fe/Mn ratio to solely identify HED parent bodies. Our estimate is very conservative since it is extremely difficult to rule out multiple HED parent bodies with similar oxygen isotopic compositions. The spread in $\Delta^{17}O$ for A-881394, Bunburra Rockhole, Emmaville, Dho 007/778, and EET 92023 is also larger than that for the typical HEDs; however, different Vesta-like bodies may have varying spreads in $\Delta^{17}O$.

While the available isotopic and geochemical evidence seems to favor seven distinct primordial HED-like asteroids (Table 1) in the main belt, this estimate comes with a caveat concerning the possible involvement of impact-related processes in modifying the bulk oxygen isotope composition of a sample. This situation is well illustrated by the howardite impact breccia Jiddat al Harasis (JaH) 556 (Janots et al., 2012). Non-HED-meteorite fragments have been found in a wide range of howardites (e.g., Buchanan et al., 1993; Lunning et al., 2016). The O-isotope bulk rock composition of JaH 556 is anomalous with respect to normal HEDs but the meteorite consists of a mixture of isotopically normal HED clasts in a vesiculated matrix containing H chondrite-derived material. The addition of H chondrite material gave the sample its anomalous bulk composition. In the case of JaH 556, the involvement of an H chondrite impactor was clear from the enhanced siderophile element content of the meteorite. However, in the case of an achondritic impactor, identifying the impact origin of the anomalous sample would be less

TABLE 1. List of HEDs or HED-like meteorites proposed to originate from different Vesta-like parent bodies.

Meteorite	$\Delta^{17}O$ (‰)	Fe/Mn (molar) ratio for low-Ca pyroxenes	Other characteristics
Typical HEDs	−0.24	29.2–33.4	NC
NWA 011/2400/2976/4587/4901	−1.6	~67	CC
Mesosiderites	−0.245	~17–35	NC; contain abundant Fe-Ni metal
Ibitira	−0.07	36.5	NC; vesicle-rich
A-881394, Bunburra Rockhole, Dho 007/778, EET 92023, Emmaville	−0.14	~31	NC; tend to have Cr isotopic compositions offset from "typical" HEDs
Pasamonte, PCA 82502/91007	−0.21	~33	NC; PCA 82502/91007 are vesicle-rich
NWA 11916	−0.44	—	Primarily pigeonite

Note: The $\Delta^{17}O$ values are from Yamaguchi et al. (2002), Floss et al. (2005), Russell et al. (2005), Greenwood et al. (2017), and Mittlefehldt et al. (2022). The Fe/Mn molar ratios are from Hibiya et al. (2019), Mittlefehldt et al. (2022), and LeLarge et al. (2022). The NC and CC (carbonaceous chondrite) designations are from Warren (2011) and Benedix et al. (2017).

straightforward. A recent study of quenched angrites, previously regarded as being free from impact-related deformation features, has shown that xenocrysts and matrix in these meteorites are in isotopic disequilibrium, most likely as a result of impact mixing (Rider-Stokes et al., 2023). In light of this, further work is needed to establish whether some anomalous HEDs were formed by impact processes on Vesta, rather than being derived from distinct parent bodies. We would note that impact rocks were likely formed in the event that produced the earlier Veneneia basin on Vesta. Such lithologies would then have been removed from Vesta during the impact event that created the Rheasilvia basin (Figure 2) and the Vesta asteroid family (Figure 4).

IRON METEORITES

Iron meteorites, primarily consisting of Fe-Ni phases, are the remnants of metallic solids that formed in the early solar system. Dawn observations (Russell et al., 2012) of Vesta indicate that it has an iron core. Based on their crystallization processes, iron meteorites can be classified as magmatic and non-magmatic types. Magmatic irons originate from the metallic cores of differentiated asteroids. These asteroids experienced core–mantle differentiation and iron meteorites from a single core have siderophile element variations consistent with fractional crystallization (Jones & Drake, 1983; Scott, 1972; Scott & Wasson, 1976; Willis & Goldstein, 1982). Fractional crystallization is the removal from a melt of early-forming mineral precipitates. Non-magmatic iron meteorites likely originated as metallic melt pools on asteroids, and these irons are formed by crystal segregation (Wasson, 2017; Wasson & Kallemeyn, 2002; Wasson & Wang, 1986). Iron meteorites have cosmic ray exposure (CRE) ages up to ~1 Ga while HEDs have CRE ages only up to ~100 Ma (Eugster, 2003), which indicates that irons can survive as meteorite-sized bodies much longer in space than HEDs.

In the magmatic iron-meteorite parent bodies, although overlaid by a silicate lid, their irons usually do not contain silicates. Except for Fe-Ni phases, magmatic irons can have sulfides (such as troilite [FeS] and daubréelite [$FeCr_2S_4$]), phosphides [schreibersite ($(Fe, Ni)_3P$)], carbides (cohenite [Fe_3C]), and oxides (chromite [$FeCr_2O_4$]) (Buchwald, 1975). In most cases, the silicate portion of magmatic iron-meteorite parent bodies might have differentiated and did not mix with the cores on a large scale. If these iron-meteorite parent bodies had survived to this day, then their silicate part might have a lithology similar to that of Vesta (a basaltic crust on top of a peridotitic mantle). In contrast, although non-magmatic irons can have abundant rock-forming silicates, such as olivine, pyroxene, and feldspar (Buchwald, 1975), these mineral phases are found to have a chondritic (undifferentiated) origin (Scott, 2020). The non-magmatic iron groups formed rapidly in the metallic melt pools and did not go through mantle–core differentiation processes. Therefore, in this study, we will primarily discuss magmatic iron meteorites.

Magmatic iron meteorites are grouped based on their elemental concentrations and metallographic structures, and members of each iron-meteorite group have similar Ga, Ge, and Ni concentrations, as well as similar textures (Goldberg et al., 1951; Lovering et al., 1957; Scott et al., 1973; Wasson, 1967, 1969, 1970a, 1970b; Wasson & Kimbeblin, 1967; Wasson & Schaudy, 1971). It has been found that Ga and Ge concentrations varied by an order of magnitude of 4 among iron-meteorite groups, and individual groups form distinctive clusters on the Ga, Ge versus Ni diagrams (Scott, 2020). Based on this classification scheme, 11 magmatic groups (member number ≥5) and a trio (so-called the South Byron trio; Table 2) have been found in our current collections. Each

of the magmatic groups/trio is derived from the metallic core of an asteroid, except that groups IIAB and IIG are believed to originate from two different layers of a single core (Wasson & Choe, 2009). Isotopic differences in elements such as Molybdenum (Mo), Nickel (Ni), and Tungsten (W) (e.g., Burkhardt et al., 2011; Kruijer et al., 2017; Nanne et al., 2019; Worsham et al., 2019) indicate that both NC and CC irons exist (Table 2). The identification of both NC and CC achondrites and NC and CC irons appears to indicate that core formation with resulting HED-like crusts occurred in both the inner and outer solar system.

The iron-meteorite parent bodies accreted less than ~1 Ma, and differentiated <4 Ma, after CAI formation (Kruijer et al., 2017; Spitzer et al., 2021). The iron-meteorite parent bodies therefore represent the earliest-formed differentiated terrestrial bodies in the solar system. After core–mantle differentiation, most of the cores were cooled under their respective insulating mantle. Thus far, no achondrites have been confidently assigned to share a common parent body with an iron-meteorite group. Pallasites are a class of stony-iron meteorites mainly composed of Fe-Ni metal and olivine (sometimes low-Ca pyroxene), and typically thought to have formed at the core–mantle boundary of differentiated asteroids (e.g., Greenberg and Chapman, 1984; Mittlefehldt et al., 1998). This scenario is now disputed and pallasites may represent assemblages formed during impact mixing (Tarduno et al., 2012; Windmill et al., 2022).

There is some evidence linking "differentiated" silicates and iron meteorites. For example, some pallasite subgroups have been linked with iron-meteorite groups. The main group pallasites, the main compositional cluster of pallasites, have been argued to have formed at the core–mantle boundary in the IIIAB parent body (Wasson & Choi, 2003). Wasson (2013) argued that even the HEDs could be related to the disrupted IIIAB parent body, instead of Vesta due to oxygen and chromium isotopic similarities; however, this similarity may just indicate that Vesta and the IIIAB parent body formed in the same region of the solar nebula. The postulated occurrence of pallasites in the IIIAB parent body would indicate that its core was likely mantled by differentiated silicates. The Milton pallasite is found to have identical elemental (siderophiles) and isotopic (Mo and Ru) compositions to the South Byron trio irons, which implies that this pallasite and the trio may share a common parent body (e.g., McCoy et al., 2019). The Eagle Station pallasites and two ungrouped low-Ca pyroxene-bearing pallasites (Zinder and NWA 1911) were first speculated to be related to groups IIF (Kracher et al., 1980) and IIIF (Zhang et al., 2022), respectively, based on the similarities in the elemental compositions of metals. However, further Mo isotopic investigations show that these two subgroups of pallasites are not genetically related to IIF (Hilton et al., 2020) or IIIF (Pape et al., 2022). Two IVA members, São João Nepomuceno and Steinbach, contain orthopyroxene, silica, and minor amounts of high-Ca pyroxene. The silicate liquids might have been ejected into the two IVA irons through shock-induced cracks (Wasson et al., 2006). If the highly evolved silicate liquids originate from the mantle, it would imply that the IVA parent body was covered by differentiated silicates. The formation of pallasites and the occurrence of evolved silicate phases in irons are good indicators for a number of iron-meteorite parent bodies being Vesta-like. For irons, "Vesta-like" indicates disrupted differentiated bodies with petrologically distinct mantles and possible HED-like crusts.

TABLE 2. List of magmatic iron groups/trio/duo and proposed magmatic irons that could potentially originate from different Vesta-like parent bodies.

Grouped or ungrouped iron	Linked group or meteorite	NC or CC
IC		NC
IIC		CC
IID		CC
IIAB/IIG		NC
IIF		CC
IIIAB	Main group pallasites	NC
IIIE		NC
IIIF		CC
IVA		NC
IVB		CC
South Byron trio	Milton pallasite	CC
Emsland/Mbosi duo		CC
Bacubirito		—
Cambria		NC
Campinorte		—
Denver City		—
Grand Rapids		CC
La Caille		CC
Laguna Manantiales		—
Morradal		—
New Baltimore		CC
Reed City		NC

Note: We also list linked pallasites (McCoy et al., 2019; Wasson & Choi, 2003) to magmatic iron groups/trio. The median Ir/Au (g g^{-1}) ratios for the magmatic iron groups are from Rubin (2018) and the Ir/Au (g g^{-1}) ratios for the trio, the duo, and the single ungrouped irons are from Wasson (2013). The Ir/Au ratio becomes highly fractionated during fractional crystallization (e.g., Wasson, 2013). The NC (non-carbonaceous) and CC (carbonaceous chondrite) designations for the magmatic iron groups are from Rubin (2018), Mbosi is from Burkhardt et al. (2011), and the South Byron trio and the ungrouped irons are from Spitzer et al. (2020).

The sizes of these iron-meteorite bodies may be comparable to those of Vesta. For example, the IVA core may have had a diameter of 150 km (Yang et al., 2008), which comprises ~20 wt% of the total mass (Hilton et al., 2022), so the IVA parent body is likely ~300 km in diameter (assuming a core density = 7.5 g cm^{-3} and a silicate density = 4.5 g cm^{-3}). The IVB parent body is estimated to have a size of ~140 km with a core of 70 km in diameter (Yang et al., 2010). The sizes of other iron-meteorite parent bodies are currently unknown due to the lack of estimates on their core sizes.

Some iron-meteorite parent bodies may not have a long-lasting thick mantle, which may not have allowed the silicate liquids to differentiate and evolve long enough into a Vesta-like lithology. Irons from a well-insulated core should have uniform cooling rates at different stages of crystallization. The earliest crystallized IVB iron has the lowest cooling rate (475 K Ma^{-1}), and the latest crystallized IVB iron has a ~10 times higher cooling rate (5000 K Ma^{-1}; Yang et al., 2010). The drastically different cooling rates for the earliest and the latest IVB irons imply that the core crystallized concentrically outward and did not have a silicate mantle (Yang et al., 2010). The mantle might have been removed by a glazing impact event with another body (Yang et al., 2010). A similar scenario was proposed for the IVA core. The earliest crystallized IVA iron has the highest cooling rate (6327 K Ma^{-1}) while the latest crystallized IVA iron has a much lower cooling rate (373 K Ma^{-1}; Yang et al., 2008). Therefore, the IVA core may have been enclosed only by a thin silicate layer and crystallized concentrically inward (Yang et al., 2008). The thermal history proposed by Yang et al. (2008) is inconsistent with the one proposed by Wasson et al. (2006), which shows that further work must be done to understand the differences in calculated cooling rates for fragments in the same iron meteorite group. If the impact had taken place much earlier before the silicate liquids were fully differentiated and evolved, the IVA and IVB parent bodies, although the mantle and the core were segregated, may not have developed a Vesta-like crust or mantle. Alternatively, if the silicate liquids were fully differentiated and evolved before the glazing impact occurred, then the IVA and IVB parent bodies would be Vesta-like. In either scenario, the mantle materials of the IVA and IVB parent bodies were destroyed within the first few million years in the solar system. A few olivine-rich meteorites that appear to be fragments of differentiated parent bodies have been discovered (Vaci et al., 2021). Other iron-meteorite cores that fully cooled under an insulated mantle may also have lost the mantle material very early in solar system history (Scott, 2020). In comparison, HEDs are typically thought to have been launched ~1 Ga ago from Vesta during the formation of the Rheasilvia basin (Schenk et al., 2022) and the resulting Vesta family (e.g., Asphaug, 1997; Carruba et al., 2007; Nesvorný et al., 2008). The very early destruction of the mantle of iron-meteorite parent bodies may also explain the scarcity of olivine-rich achondrites in our collections (Burbine et al., 1996; Scott, 2020). Olivine-dominated asteroids, usually classified as A-types, are also rare in the asteroid belt (DeMeo et al., 2019).

Aside from the aforementioned iron-meteorite groups, there are also over 150 recorded ungrouped iron meteorites (Meteoritical Bulletin Database, 2024) that cannot fit into the current groups plus ~100 iron meteorites that have not been classified. Wasson (2013) speculated that half of the current ungrouped iron meteorites might belong to the IAB complex. Because most ungrouped iron meteorites do not form fractional crystallization trend lines, Wasson (2013) established new compositional criteria to evaluate whether ungrouped (or unclassified) iron meteorites are magmatic. These criteria were that the (1) Mass ⩾1.9 kg; (2) Ir/Au ratios ⩽1.0 or ⩾9 g g^{-1}; and (3) textures that implied slow cooling. Large or small Ir/Au ratios were chosen as a way to identify magmatic irons due to fractional crystallization producing large fractionations in this ratio (Wasson, 2013). Irons that formed through fractional crystallization would be expected to have Ir/Au ratios that differ significantly from the chondritic ratio. Using these criteria, Wasson (2013) concluded that at least 10 magmatic parent bodies (Table 2) can be inferred from the current ungrouped (or unclassified) iron meteorites. We have removed ungrouped irons that have been subsequently classified as part of one of the magmatic iron groups so our ungrouped magmatic iron number is lower than the number given by Wasson (2013). Wasson (2013) also identified the South Byron trio and Emsland/Mbosi duo as being magmatic. Thus far, the morphology and redox conditions of the ungrouped iron-meteorite-related parent bodies are unknown, but these asteroids may be Vesta-like.

However, the existence of non-HED crustal/mantle material in our meteorite collections almost certainly implies that not all known magmatic irons had Vesta-like crusts. Angrites (e.g., Zhu et al., 2019), aubrites (e.g., Casanova et al., 1993), and andesitic meteorites such as Graves Nunatak (GRA) 06128/06129 (Day et al., 2009), NWA 11119 (Srinivasan et al., 2018), and Erg Chech (EC) 002 (Niclas et al. 2022) are all believed to possibly be crustal/mantle material that would be expected to have formed on bodies with iron cores. However, Anand et al. (2022) argue that EC 002 is a crustal fragment from a parent body of an undiscovered magmatic iron group due to isotopic ($\varepsilon^{54}Cr$ and $\Delta^{17}O$) differences between EC 002 and known magmatic irons. It is extremely difficult to link an achondrite to a particular magmatic iron

meteorite or iron meteorite group since these irons tend not to contain fragments of the mantle or crust. Modeling (e.g., Grewal et al., 2022) is underway to try to link iron meteorites and crustal material using partition coefficients for different elements.

In summary, all magmatic iron-meteorite parent bodies appeared to have gone through core–mantle differentiation processes, so these parent bodies could possibly be Vesta-like objects, especially the groups/trio that may have related pallasites (e.g., IIIAB, the South Byron trio) or highly evolved silicate phases (e.g., IVA). Non-magmatic iron-meteorite groups (IAB and IIE) crystallized rapidly from metallic melt pools on asteroids, and neither of these two groups formed Vesta-like bodies. The sizes of many iron-meteorite parent bodies may also be at the same scale as that of Vesta. The mantles of iron-meteorite parent bodies may have been destroyed very early in solar system history, which could be one of the reasons that we, so far, have found limited potential mantle material from iron-meteorite parent bodies. We conclude that there are potentially up to 22 Vesta-like asteroids inferred from iron meteorites with 10 accounting for the established magmatic iron groups, one for the South Byron trio, and one for the Emsland/Mbosi duo plus 10 accounting for the ungrouped irons. When we include Vesta, we postulate that there were potentially as many as 23 Vesta-like bodies. However, this number is most likely an overestimation of the number of Vesta-like bodies due to the existence of a number of non-HED crustal/mantle material such as angrites, aubrites, and andesitic meteorites that potentially originated from bodies with magmatic iron cores.

CONCLUSIONS

Francis Galton (1822–1911) found that the median and mean of the guesses of a weight-judging competition for an ox better represented the true weight than the closest guess (Wallis, 2014). Using that study as a guide, we will take the average number of "guesses" for the number of Vesta-like bodies from our different types of evidence as the "best" number. We assume two Vesta-like bodies once existed from the astronomical evidence; seven from the isotopic, chemical, and petrologic evidence; and 23 from the iron meteorite evidence.

Since it is hard to justify an exact number due to all the uncertainties in our analyses, we estimate that there were 10 or so Vesta-like bodies that once existed in the main belt. The astronomical and the isotopic, chemical, and petrologic evidence give insight on the number of Vesta-like crusts that formed while the iron meteorite evidence gives information on the number of disrupted cores that formed. Most likely, the astronomical evidence is underestimating the number of Vesta-like parent bodies due to the difficulty identifying the original parent body of thousands of V-type bodies while the iron meteorite evidence is most certainly overestimating the number. Not all magmatic iron cores would be expected to have HED crusts. The isotopic, chemical, and petrologic evidence could be underestimating or overestimating the number of Vesta-like bodies. Crustal material would be easier to break down than Fe-Ni metal so iron meteorites would be expected to have a higher probability to survive to the present day. However, impact contamination could be potentially altering the oxygen isotopic composition of some HED meteorites, which would inflate the number of predicted Vesta-like bodies.

To really refine these estimates, further work must be done. More V-types need to be spectrally observed in the near-infrared region. More modeling needs to be done to constrain how far fragments from Vesta could have drifted from early in solar system history to the formation of the Vesta family. Oxygen isotopic analyses should be done on all HEDs to try to constrain how many of these meteorites are anomalous and whether there are any mineralogical or chemical traits that link anomalous HEDs together. Further work needs to be done on iron meteorites to try to constrain their crust and mantle compositions of these disrupted parent bodies. Future siderophile elemental and isotopic analyses of currently and newly found achondrites may allow us to test how much mantle material survived through solar system history and give better constraints on whether these bodies were Vesta-like. Sample return missions from V-type bodies would help to answer many of these questions on the variety of mineralogical, chemical, and isotopic properties of these objects.

Our preferred scenario is that approximately 10 Vesta-like objects formed early in solar system history and all but Vesta were disrupted. Vesta got extremely "lucky" and survived two large impacts at its south pole that resulted in the Rheasilvia and Veneneia basins but surprisingly did not break apart the whole body. The disrupted bodies had their crusts and mantles pulverized, which resulted in a relatively small number of crustal fragments surviving as meteorites or asteroids until the present day. Our meteorite collections and the inner main belt are filled with fragments of Vesta due to the relatively recent impact that formed the Rheasilvia basin.

Acknowledgments—This paper is dedicated to the memory of Edward R. D. Scott (1947–2021) who was a pioneer in the study of iron meteorites. THB would like to thank the Remote, In Situ, and Synchrotron Studies for Science and Exploration 2 (RISE2) and Solar System Exploration Research Virtual Institute (SSERVI) (NASA grant 80NSSC19M0215) for support. BZ would like to thank NASA grants 80NSSC19K1238 and 80NSSC23K0035

for support. This research has made use of the Asteroid Families Portal maintained at the Department of Astronomy/University of Belgrade. Asteroid reflectance spectra were downloaded from the NASA Planetary Data Systems (PDS). This research utilizes meteorite reflectance spectra acquired at the NASA RELAB facility at Brown University.

Data Availability Statement—The data that support the findings of this study are openly available in the RELAB Spectral Library Bundle at https://doi.org/10.17189/1519032, the Small Main-belt Asteroid Spectroscopic Survey, Phase II at https://sbnapps.psi.edu/ferret/datasetDetail.action?dataSetId=EAR-A-I0028-4-SBN0001%2FSMASSII-V1.0, the Reddy Main Belt Asteroid Spectra V1.0 at https://sbnapps.psi.edu/ferret/datasetDetail.action?dataSetId=EAR-A-I0046-3-REDDYMBSPEC-V1.0, the IRTF Near-IR Spectroscopy of Asteroids V2.0 at https://sbnapps.psi.edu/ferret/datasetDetail.action?dataSetId=EAR-A-I0046-4-IRTFSPEC-V2.0, the Small Solar System Objects Spectroscopic Survey V1.0 at https://sbnapps.psi.edu/ferret/datasetDetail.action?dataSetId=EAR-A-I0052-8-S3OS2-V1.0, the Hardersen IRTF Asteroid NIR Reflectance Spectra V1.0 at https://sbnapps.psi.edu/ferret/datasetDetail.action?dataSetId=EAR-A-I0046-3-HARDERSENSPEC-V1.0, the Asteroid Families Portal at http://asteroids.matf.bg.ac.rs/fam/, the Nesvorny HCM Asteroid Families V3.0 at https://sbnapps.psi.edu/ferret/datasetDetail.action?dataSetId=EAR-A-VARGBDET-5-NESVORNYFAM-V3.0, and the Asteroid Taxonomy V6.0 at https://sbnapps.psi.edu/ferret/datasetDetail.action?dataSetId=EAR-A-5-DDR-TAXONOMY-V6.0.

Editorial Handling—Dr. Edward Anthony Cloutis

REFERENCES

Alvarez-Candal, A., Duffard, R., Lazzaro, D., and Michtchenko, T. 2006. The Inner Region of the Asteroid Main Belt: A Spectroscopic and Dynamic Analysis. *Astronomy & Astrophysics* 459: 969–976.

Anand, A., Kruttasch, P. M., and Mezger, K. 2022. ^{53}Mn-^{53}Cr Chronology and ε^{54}Cr-Δ^{17}O Genealogy of Erg Chech 002: The Oldest Andesite in the Solar System. *Meteoritics & Planetary Science* 57: 2003–16.

Angrisani, M., Palomba, E., Longobardo, A., Raponi, A., Dirri, F., and Gisellu, C. 2023. A New Prospect to Analyse the Spectral Properties of V-Type Asteroids. *Icarus* 390: 115320.

Asphaug, E. 1997. Impact Origin of the Vesta Family. *Meteoritics & Planetary Science* 32: 965–980.

Barrat, J. A., Jambon, A., Bohn, M., Blichert-Toft, J., Sautter, V., Göpel, C., Gillet, P., Boudouma, O., and Keller, F. 2003. Petrology and Geochemistry of the Unbrecciated Achondrite Northwest Africa 1240 (NWA 1240): An HED Parent Body Impact Melt. *Geochimica et Cosmochimica Acta* 67: 3959–70.

Barrett, T. J., Mittlefehldt, D. W., Greenwood, R. C., Charlier, B. L. A., Hammond, S. J., Ross, D. K., Anand, M., Franchi, I. A., Abernethy, F. A. J., and Grady, M. M. 2017. The Mineralogy, Petrology, and Composition of Anomalous Eucrite Emmaville. *Meteoritics & Planetary Science* 52: 656–668.

Benedix, G. K., Bland, P. A., Friedrich, J. M., Mittlefehldt, D. W., Sanborn, M. E., Yin, Q.-Z., Greenwood, R. C., et al. 2017. Bunburra Rockhole: Exploring the Geology of a New Differentiated Asteroid. *Geochimica et Cosmochimica Acta* 208: 145–159.

Binzel, R. P., and Xu, S. 1993. Chips off of Asteroid 4 Vesta: Evidence for the Parent Body of Basaltic Achondrite Meteorites. *Science* 260: 186–191.

Brasil, P. I. O., Roig, F., Nesvorný, D., and Carruba, V. 2017. Scattering V-Type Asteroids during the Giant Planet Instability: A Step for Jupiter, a Leap for Basalt. *Monthly Notices of the Royal Astronomical Society* 468: 1236–44.

Buchanan, P. C., Zolensky, M. E., and Reid, A. M. 1993. Carbonaceous Chondrite Clasts in the Howardites Bholghati and EET87513. *Meteoritics & Planetary Science* 28: 659–669.

Buchwald, V. F. 1975. *Handbook of Iron Meteorites. Their History, Distribution, Composition and Structure, Volumes 1–3*. Berkeley: University of California Press.

Burbine, T. H., Buchanan, P. C., Binzel, R. P., Bus, S. J., Hiroi, T., Hinrichs, J. L., Meibom, A., and McCoy, T. J. 2001. Vesta, Vestoids, and the Howardite, Eucrite, Diogenite Group: Relationships and the Origin of Spectral Differences. *Meteoritics & Planetary Science* 36: 761–781.

Burbine, T. H., Buchanan, P. C., Jercinovic, M. J., and Greenwood, R. C. 2023. Determining the Pyroxene Mineralogies of Vestoids. *Planetary Science Journal* 4: 96.

Burbine, T. H., Duffard, R., Buchanan, P. C., Cloutis, E. A., and Binzel, R. P. 2011. Spectroscopy of O-Type Asteroids. *42nd Lunar and Planetary Science Conference*, abstract #2483.

Burbine, T. H., McCoy, T. J., Hinrichs, J. L., and Lucey, P. G. 2006. Spectral Properties of Angrites. *Meteoritics & Planetary Science* 41: 1139–45.

Burbine, T. H., McCoy, T. J., Nittler, L. R., Benedix, G. K., Cloutis, E. A., and Dickinson, T. L. 2002. Spectra of Extremely Reduced Assemblages: Implications for Mercury. *Meteoritics & Planetary Science* 37: 1233–44.

Burbine, T. H., Meibom, A., and Binzel, R. P. 1996. Mantle Material in the Main Belt: Battered to Bits? *Meteoritics & Planetary Science* 31: 607–620.

Burbine, T. H., Wallace, S. M., and Dyar, M. D. 2019. Applying the Bus-DeMeo Asteroid Taxonomy to Meteorite Spectra. *50th Lunar and Planetary Science Conference*, abstract #1655.

Burkhardt, C., Kleine, T., Oberli, F., Pack, A., Bourdon, B., and Wieler, R. 2011. Molybdenum Isotope Anomalies in Meteorites: Constraints on Solar Nebula Evolution and Origin of the Earth. *Earth and Planetary Science Letters* 312: 390–400.

Bus, S., and Binzel, R. P. 2003. Small Main-belt Asteroid Spectroscopic Survey, Phase II. EAR-A-I0028-4-SBN0001/SMASSII-V1.0. NASA Planetary Data System.

Bus, S. J. 2011. Near_IR Spectrum of Asteroid 1929 Kollaa. EAR-A-I0046-4-IRTFSPEC-V2.0:MOSKOVITZETAL2010_1929_010219T133209_TAB. NASA Planetary Data System.

Bus, S. J., and Binzel, R. P. 2002a. Phase II of the Small Main-Belt Asteroid Spectroscopic Survey: The Observations. *Icarus* 158: 106–145.

Bus, S. J., and Binzel, R. P. 2002b. Phase II of the Small Main-Belt Asteroid Spectroscopic Survey: A Feature-Based Taxonomy. *Icarus* 158: 146–177.

Carruba, V., Huaman, M. E., Domingos, R. C., Dos Santos, C. R., and Souami, D. 2014. Dynamical Evolution of V-Type Asteroids in the Central Main Belt. *Monthly Notices of the Royal Astronomical Society* 439: 3168–79.

Carruba, V., Michtchenko, T. A., Roig, F., Ferraz-Mello, S., and Nesvorný, D. 2005. On the V-Type Asteroids Outside the Vesta Family I. Interplay of Nonlinear Secular Resonances and the Yarkovsky Effect: The Cases of 956 Elisa and 809 Lundia. *Astronomy & Astrophysics* 441: 819–829.

Carruba, V., Roig, F., Michtchenko, T. A., Ferraz-Mello, S., and Nesvorný, D. 2007. Modeling Close Encounters with Massive Asteroids: A Markovian Approach. An Application to the Vesta Family. *Astronomy & Astrophysics* 465: 315–330.

Carruba, V., Vokrouhlický, D., and Novaković, B. 2018. Asteroid Families Interacting with Secular Resonances. *Planetary and Space Science* 157: 72–81.

Carvano, J. M., Hasselmann, P. H., Lazzaro, D., and Mothé-Diniz, T. 2010. SDSS-Based Taxonomic Classification and Orbital Distribution of Main Belt Asteroids. *Astronomy & Astrophysics* 510: A43.

Casanova, I., Keil, K., and Newsom, H. E. 1993. Composition of Metal in Aubrites: Constraints on Core Formation. *Geochimica et Cosmochimica Acta* 57: 675–682.

Clayton, R. N. 2003. Oxygen Isotopes in the Solar System. *Space Science Reviews* 106: 19–32.

Colazo, M., Alvarez-Candal, A., and Duffard, R. 2022. Zero-Phase Angle Asteroid Taxonomy Classification Using Unsupervised Machine Learning Algorithms. *Astronomy & Astrophysics* 666: A77.

Correa-Otto, J. A., and Cañada-Assandri, M. 2018. Dynamic Portrait of the Region Occupied by the Hungaria Asteroids: The Influence of Mars. *Monthly Notices of the Royal Astronomical Society* 479: 1694–1701.

Day, J. M. D., Ash, R. D., Liu, Y., Bellucci, J. J., Rumble, D., III, McDonough, W. F., Walker, R. J., and Taylor, L. A. 2009. Early Formation of Evolved Asteroidal Crust. *Nature* 457: 179–182.

Delbo, M., Gai, M., Lattanzi, M. G., Ligori, S., Loreggia, D., Saba, L., Cellino, A., et al. 2006. MIDI Observations of 1459 Magnya: First Attempt of Interferometric Observations of Asteroids with the VLTI. *Icarus* 181: 618–622.

DeMeo, F., Binzel, R. P., Slivan, S. M., and Bus, S. J. 2009. An Extension of the Bus Asteroid Taxonomy into the Near-Infrared. *Icarus* 202: 160–180.

DeMeo, F. E., Polishook, D., Carry, B., Burt, B. J., Hsieh, H. H., Binzel, R. P., Moskovitz, N. A., and Burbine, T. H. 2019. Olivine-Dominated A-Type Asteroids in the Main Belt: Distribution, Abundance and Relation to Families. *Icarus* 322: 13–30.

Duffard, R., Lazzaro, D., Licandro, J., De Sanctis, M. C., Capria, M. T., and Carvano, J. M. 2004. Mineralogical Characterization of some Basaltic Asteroids in the Neighborhood of (4) Vesta: First Results. *Icarus* 171: 120–132.

Eugster, O. 2003. Cosmic-Ray Exposure Ages of Meteorites and Lunar Rocks and their Significance. *Geochemistry* 63: 3–30.

Floss, C., Taylor, L. A., Promprated, P., and Rumble, D., III. 2005. Northwest Africa 011: A "Eucritic" Basalt from a Non-eucrite Parent Body. *Meteoritics & Planetary Science* 40: 343–360.

Goldberg, E., Uchiyama, A., and Brown, H. 1951. The Distribution of Nickel, Cobalt, Gallium, Palladium and Gold in Iron Meteorites. *Geochimica et Cosmochimica Acta* 2: 1–25.

Greenberg, R., and Chapman, C. R. 1984. Asteroids and Meteorites: Origin of Stony-Iron Meteorites at Mantle-Core Boundaries. *Icarus* 57: 267–279.

Greenwood, R. C., Burbine, T. H., and Franchi, I. A. 2020. Linking Asteroids and Meteorites to the Primordial Planetesimal Population. *Geochimica et Cosmochimica Acta* 277: 377–406.

Greenwood, R. C., Burbine, T. H., Miller, M. F., and Franchi, I. A. 2017. Melting and Differentiation of Early-Formed Asteroids: The Perspective from High Precision Oxygen Isotope Studies. *Geochemistry* 77: 1–43.

Greenwood, R. C., Franchi, I. A., Jambon, A., Barrat, J. A., and Burbine, T. H. 2006. Oxygen Isotope Variation in Stony-Iron Meteorites. *Science* 313: 1763–65.

Greenwood, R. C., Franchi, I. A., Jambon, A., and Buchanan, P. C. 2005. Widespread Magma Oceans on Asteroidal Bodies in the Early Solar System. *Nature* 435: 916–18.

Grewal, D. S., Seales, J. D., and Dasgupta, R. 2022. Internal or External Magma Oceans in the Earliest Protoplanets—Perspectives from Nitrogen and Carbon Fractionation. *Earth and Planetary Science Letters* 598: 117847.

Haba, M. K., Wotzlaw, J.-F., Lai, Y.-J., Yamaguchi, A., and Schönbächler, M. 2019. Mesosiderite Formation on Asteroid 4 Vesta by a Hit-and-Run Collision. *Nature Geosciences* 12: 510–15.

Hardersen, P. S. 2016. Hardersen IRTF Asteroid NIR Reflectance Spectra V1.0. EAR-A-I0046-3-HARDERSENSPEC-V1.0. NASA Planetary Data System.

Hardersen, P. S., Gaffey, M. J., and Abell, P. A. 2004. Mineralogy of Asteroid 1459 Magnya and Implications for its Origin. *Icarus* 167: 170–77.

Hardersen, P. S., Reddy, V., Cloutis, E., Nowinski, M., Dievendorf, M., Genet, R. M., Becker, S., and Roberts, R. 2018. Basalt or Not? Near-Infrared Spectra, Surface Mineralogical Estimates, and Meteorite Analogs for 33 V_p-Type Asteroids. *Astronomical Journal* 156: 11.

Hardersen, P. S., Reddy, V., and Roberts, R. 2015. Vestoids, Part II: The Basaltic Nature and HED Meteorite Analogs for Eight V_p-Type Asteroids and their Associations with (4) Vesta. *Astrophysical Journal Supplement Series* 221: 19.

Hardersen, P. S., Reddy, V., Roberts, R., and Mainzer, A. 2014. More Chips off of Asteroid (4) Vesta: Characterization of Eight Vestoids and their HED Meteorite Analogs. *Icarus* 242: 269–282.

Hibiya, Y., Archer, G. J., Tanaka, R., Sanborn, M. E., Sato, Y., Iizuka, T., Ozawa, K., et al. 2019. Mineralogical Criteria for the Parent Asteroid of the "Carbonaceous" Achondrite NWA 6704. *Geochimica et Cosmochimica Acta* 107: 135–154.

Hicks, M. D., Buratti, B. J., Lawrence, K. J., Hillier, J., Li, J.-Y., Reddy, V., Schröder, S., et al. 2014. Spectral Diversity and Photometric Behavior of Main-Belt and Near-Earth Vestoids and (4) Vesta: A Study in Preparation for the Dawn Encounter. *Icarus* 235: 60–74.

Hilton, C. D., Ash, R. D., and Walker, R. J. 2020. Crystallization Histories of the Group IIF Iron Meteorites and Eagle Station Pallasites. *Meteoritics & Planetary Science* 55: 2570–86.

Hilton, C. D., Ash, R. D., and Walker, R. J. 2022. Chemical Characteristics of Iron Meteorite Parent Bodies. *Geochimica et Cosmochimica Acta* 318: 112–125.

Hiroi, T., Binzel, R. P., Sunshine, J. M., Pieters, C. M., and Takeda, H. 1995. Grain Sizes and Mineral Compositions of Surface Regoliths of Vesta-Like Asteroids. *Icarus* 115: 374–386.

Hiroi, T., Pieters, C. M., and Takeda, H. 1994. Grain Size of the Surface Regolith of Asteroid 4 Vesta Estimated from its Reflectance Spectrum in Comparison with HED Meteorites. *Meteoritics & Planetary Science* 29: 394–96.

Huaman, M. E., Carruba, V., and Domingos, R. C. 2014. Dynamical Evolution of V-Type Photometric Candidates in the Outer Main Belt. *Monthly Notices of the Royal Astronomical Society* 444: 2985–92.

Janots, E., Gnos, E., Hofmann, B., Greenwood, R. C., Franchi, I. A., Bermingham, K., and Netwing, V. 2012. Jiddat al Harasis 556: A Howardite Impact Breccias with an H Chondrite Component. *Meteoritics & Planetary Science* 47: 1558–74.

Jones, J. H., and Drake, M. J. 1983. Experimental Investigations of Trace Element Fractionation in Iron Meteorites, II: The Influence of Sulfur. *Geochimica et Cosmochimica Acta* 47: 1199–1209.

Jurewicz, A. J. G., Mittlefehldt, D. W., and Jones, J. H. 1991. Partial Melting of the Allende (CV3) Meteorite: Implications for Origins of Basaltic Meteorites. *Science* 252: 695–98.

Jurewicz, A. J. G., Mittlefehldt, D. W., and Jones, J. H. 1993. Experimental Partial Melting of the Allende (CV) and Murchison (CM) Chondrites and the Origin of Asteroidal Basalts. *Geochimica et Cosmochimica Acta* 57: 2123–39.

Khanani, I., Kumawat, D., Hussain, A., Burbine, T. H., Wallace, S. M., and Dyar, M. D. 2021. Mineralogically Testing the Bus-DeMeo Taxonomy Using Meteorite Spectra (abstract). *Bulletin of the American Astronomical Society* 53: 2021n7i306p18.

Kleine, T., Budde, G., Burkhardt, C., Kruijer, T. S., Worsham, E. A., Morbidelli, A., and Nimmo, F. 2020. The Non-Carbonaceous–Carbonaceous Meteorite Dichotomy. *Space Science Reviews* 216: 55.

Kracher, A., Willis, J., and Wasson, J. T. 1980. Chemical Classification of Iron Meteorites—IX. A New Group (IIF), Revision of IAB and IIICD, and Data on 57 Additional Irons. *Geochimica et Cosmochimica Acta* 44: 773–787.

Kruijer, T. S., Burkhardt, C., Budde, G., and Kleine, T. 2017. Age of Jupiter Inferred from the Distinct Genetics and Formation Times of Meteorites. *Proceedings of the National Academy of Sciences of the United States of America* 114: 6712–16.

Larson, H. P., and Fink, U. 1975. Infrared Spectral Observations of Asteroid 4 Vesta. *Icarus* 26: 420–27.

Lazzaro, D., Angeli, C. A., Carvano, J. M., Mothe-Diniz, T., Duffard, R., and Florczak, M. 2004. S_3OS_2: The Visible Spectroscopic Survey of 820 Asteroids. *Icarus* 172: 179–220.

Lazzaro, D., Angeli, C. A., Carvano, J. M., Mothe-Diniz, T., Duffard, R., and Florczak, M. 2006. Small Solar System Objects Spectroscopic Survey V1.0. EAR-A-I0052-8-S3OS2-V1.0. NASA Planetary Data System.

Lazzaro, D., Michtchenko, T., Carvano, J. M., Binzel, R. P., Bus, S. J., Burbine, T. H., Mothé-Diniz, T., Florczak, M., Angeli, C. A., and Harris, A. W. 2000. Discovery of a Basaltic Asteroid in the Outer Main Belt. *Science* 288: 2033–35.

LeLarge, S. I., Folco, L. M., Masotta, M., Greenwood, R. C., Russell, S. S., and Bates, H. C. 2022. Asteroids Accretion, Differentiation, and Break-Up in the Vesta Source Region: Evidence from Cosmochemistry of Mesosiderites. *Geochimica et Cosmochimica Acta* 329: 135–151.

Licandro, J., Popescu, M., Morate, D., and de León, J. 2017. V-Type Candidates and Vesta Family Asteroids in the Moving Objects VISTA (MOVIS) Catalogue. *Astronomy & Astrophysics* 600: A126.

Lovering, J. F., Nichiporuk, W., Chodos, A., and Brown, H. 1957. The Distribution of Gallium, Germanium, Cobalt, Chromium, and Copper in Iron and Stony-Iron Meteorites in Relation to Nickel Content and Structure. *Geochimica et Cosmochimica Acta* 11: 263–278.

Lucas, M. P., Emery, J. P., Hiroi, T., and McSween, H. Y. 2019. Spectral Properties and Mineral Compositions of Acapulcoite-Lodranite Clan Meteorites: Establishing S-Type Asteroid-Meteorite Connections. *Meteoritics & Planetary Science* 54: 157–180.

Lunning, N. G., Welten, K. C., McSween, H. Y., Caffee, M. W., and Beck, A. W. 2016. Grosvenor Mountains 95 Howardite Pairing Group: Insights into the Surface Regolith of Asteroid 4 Vesta. *Meteoritics & Planetary Science* 51: 167–194.

Mandler, B. E., and Elkins-Tanton, L. T. 2013. The Origin of Eucrites, Diogenites, and Olivine Diogenites: Magma Ocean Crystallization and Shallow Magma Chamber Processes on Vesta. *Meteoritics & Planetary Science* 48: 2333–49.

Mansour, J.-A., Popescu, M., de León, J., and Licandro, J. 2020. Distribution and Spectrophotometric Classification of Basaltic Asteroids. *Monthly Notices of the Royal Astronomical Society* 491: 5966–79.

Matlovič, P., de Leon, J., Medeiros, H., Popescu, M., Rizos, J. L., and Mansour, J.-A. 2020. Spectral Characterisation of 14 V-Type Candidate Asteroids from the MOVIS Catalogue. *Astronomy & Astrophysics* 643: A107.

McCord, T. B., Adams, J. B., and Johnson, T. V. 1970. Asteroid Vesta: Spectral Reflectivity and Compositional Implications. *Science* 168: 1445–47.

McCoy, T. J., Corrigan, C. M., Nagashima, K., Reynolds, V. S., Ash, R. D., McDonough, W. F., Yang, J., Goldstein, J. I., and Hilton, C. D. 2019. The Milton Pallasite and South Byron Trio Irons: Evidence for Oxidation and Core Crystallization. *Geochimica et Cosmochimica Acta* 259: 358–370.

McCoy, T. J., Ketcham, R. A., Wilson, L., Benedix, G. K., Wadhwa, M., and Davis, A. M. 2005. Formation of Vesicles in Asteroidal Basaltic Meteorites. *Earth and Planetary Science Letters* 246: 102–8.

McGraw, A. M., Reddy, V., Izawa, M. R. M., Sanchez, J. A., Le Corre, L., Cloutis, E. A., Applin, D. M., and Pearson, N. 2020. Mineralogical Criteria for the Parent Asteroid of the "Carbonaceous" Achondrite NWA 6704. *Astronomical Journal* 159: 107.

McSween, H. Y., Binzel, R. P., de Sanctis, M. C., Ammannito, E., Prettyman, T. H., Beck, A. W., Reddy, V., et al. 2014. Dawn; the Vesta-HED Connection; and the Geologic Context for Eucrites, Diogenites, and Howardites. *Meteoritics & Planetary Science* 48: 2090–2104.

Meteoritical Bulletin Database 2024. https://www.lpi.usra.edu/meteor/.

Michtchenko, T. A., Lazzaro, D., Ferraz-Mello, S., and Roig, F. 2002. Origin of the Basaltic Asteroid 1459 Magnya: A Dynamical and Mineralogical Study of the Outer Main Belt. *Icarus* 158: 343–359.

Miller, M. F. 2002. Isotopic Fractionation and the Quantification of ^{17}O Anomalies in the Oxygen Three-Isotope System: An

Appraisal and Geochemical Significance. *Geochimica Cosmochimica Acta* 66: 1881–89.
Mittlefehldt, D. W. 1990. Petrogenesis of Mesosiderites: I. Origin of Mafic Lithologies and Comparison with Basaltic Achondrites. *Geochimica et Cosmochimica Acta* 54: 1165–73.
Mittlefehldt, D. W. 2005. Ibitira: A Basaltic Achondrite from a Distinct Parent Asteroid and Implications for the Dawn Mission. *Meteoritics & Planetary Science* 40: 665–677.
Mittlefehldt, D. W., Berger, E. L., and Le, L. 2017. Petrology of Anomalous Mafic Achondrite Polymict Breccia Pasamonte. *48th Lunar and Planetary Science Conference*, abstract #1194.
Mittlefehldt, D. W., Greenwood, R. C., Berger, E. L., Le, L., Peng, Z. X., and Ross, D. K. 2022. Eucrite-Type Achondrites: Petrology and Oxygen Isotope Compositions. *Meteoritics & Planetary Science* 57: 484–526.
Mittlefehldt, D. W., and Lindstrom, M. M. 1993. Geochemistry of Eucrites: Genesis of Basaltic Eucrites, and Hf and Ta as Petrogenetic Indicators for Altered Antarctic Eucrites. *Geochimica et Cosmochimica Acta* 67: 1911–34.
Mittlefehldt, D. W., McCoy, T. J., Goodrich, C. A., and Kracher, A. 1998. Non-Chondritic Meteorites from Asteroidal Bodies. In *Reviews in Mineralogy: Planetary Materials*, edited by J. Papike, vol. 36, 4-1–4-195. Washington, DC: Mineralogical Society of America.
Moskovitz, N. A., Lawrence, S., Jedicke, R., Ma, W., Haghighipour, N., Bus, S. J., and Gaidos, E. 2008. A Spectroscopically Unique Main-Belt Asteroid: 10537 (1991 RY_{16}). *Astrophysical Journal Letters* 682: L57–L60.
Moskovitz, N. A., Willman, M., Burbine, T. H., Binzel, R. P., and Bus, S. J. 2010. A Spectroscopic Comparison of HED Meteorites and V-Type Asteroids in the Inner Main Belt. *Icarus* 208: 773–788.
Nanne, J. A. M., Nimmo, F., Cuzzi, J. N., and Kleine, T. 2019. Origin of the Non-Carbonaceous–Carbonaceous Meteorite Dichotomy. *Earth and Planetary Science Letters* 511: 44–54.
Nesvorny, D. 2015. Nesvorny HCM Asteroid Families V3.0. EAR-A-VARGBDET-5-NESVORNYFAM-V3.0. NASA Planetary Data System.
Nesvorný, D., Roig, F., Gladman, B., Lazzaro, D., Carruba, V., and Mothé-Dini, T. 2008. Fugitives from the Vesta Family. *Icarus* 193: 85–95.
Nicklas, R. W., Day, J. M. D., Gardner-Vandy, K. G., and Udry, A. 2022. Early Silicic Magmatism on a Differentiated Asteroid. *Nature Geoscience* 15: 696–99.
Novaković, B., Vokrouhlický, D., Spoto, F., and Nesvorný, D. 2022. Asteroid Families: Properties, Recent Advances and Future Opportunities. *Celestial Mechanics and Dynamical Astronomy* 134: 34.
Oszkiewicz, D., Klimczak, H., Carry, B., Penttilä, A., Popescu, M., Kruger, J., and Keniger, M. A. 2023. Spectral Analysis of Basaltic Asteroids Observed by the Gaia Space Mission. *Monthly Notices of the Royal Astronomical Society* 519: 2917–28.
Oszkiewicz, D., Troianskyi, V., Föhring, D., Galád, A., Kwiatkowski, T., Marciniak, A., Skiff, B. A., et al. 2020. Spin Rates of V-Type Asteroids. *Astronomy & Astrophysics* 643: A117.
Pang, R. L., Du, W., Zhang, A. C., Liu, J., and Qin, L. 2020. Unique Achondrite Dhofar 778: A Mantle-Derived Fragment from a New Differentiated Body? *51st Lunar and Planetary Science Conference*, abstract #1947.
Pape, J., Zhang, B., Spitzer, F., Rubin, A. E., and Kleine, T. 2022. Tungsten and Molybdenum Isotopic Constraints on the Origin and Chronology of IIIF Iron Meteorites. 85th Annual Meeting of the Meteoritical Society, abstract #6478.
Papike, J. J., Karner, J. M., and Shearer, C. K. 2003. Determination of Planetary Basalt Parentage: A Simple Technique Using the Electron Microprobe. *American Mineralogist* 88: 469–472.
Reddy, V., and Sanchez, J. A. 2016. Reddy Main Belt Asteroid Spectra V1.0. EAR-A-I0046-3-REDDYMBSPEC-V1.0. NASA Planetary Data System.
Rider-Stokes, B. G., Greenwood, R. C., Anand, M., White, L. F., Franchi, I. A., Debaille, V., Goderis, S., et al. 2023. Evidence for Impact Mixing among Rocky Planetesimals in the Early Solar System from Angrite Oxygen Isotopes. *Nature Astronomy* 7: 836–842. https://doi.org/10.1038/s41550-023-01968-0.
Righter, K., and Drake, M. J. 1997. A Magma Ocean on Vesta: Core Formation and Petrogenesis of Eucrites and Diogenites. *Meteoritics & Planetary Science* 32: 929–944.
Roig, F., and Gil-Hutton, R. 2006. Selecting Candidate V-Type Asteroids from the Analysis of the Sloan Digital Sky Survey Colors. *Icarus* 183: 411–19.
Roig, F., Nesvorný, D., Gil-Hutton, R., and Lazzaro, D. 2008. V-Type Asteroids in the Middle Main Belt. *Icarus* 194: 125–136.
Rubin, A. E. 2018. Carbonaceous and Noncarbonaceous Iron Meteorites: Differences in Chemical, Physical, and Collective Properties. *Meteoritics & Planetary Science* 53: 2357–71.
Russell, C. T., Raymond, C. A., Coradini, A., McSween, H. Y., Zuber, M. T., Nathues, A., De Sanctis, M. C., et al. 2012. Dawn at Vesta: Testing the Protoplanetary Paradigm. *Science* 336: 684–86.
Russell, S. S., Zolensky, M., Righter, K., Folco, L., Jones, R., Connolly, H. C., Jr., Grady, M. M., and Grossman, J. N. 2005. The Meteoritical Bulletin, No. 89, 2005 September. *Meteoritics & Planetary Science* 40: A201–A263.
Ruzicka, A., Grossman, J. N., and Garvie, L. 2014. The Meteoritical Bulletin, No. 100. *Meteoritics & Planetary Science* 49: E1–E101.
Ruzicka, A., Snyder, G. A., and Taylor, L. A. 1997. Vesta as the HED Parent Body: Implications for the Size of a Core and for Large-Scale Differentiation. *Meteoritics & Planetary Science* 32: 825–840.
Sanborn, M. E., Yin, Q.-Z., Amelin, Y., Koefoed, P., and Huyskens, M. 2018. Early Differentiation of Carbonaceous Achondrite Parent Bodies: New Insights from Northwest Africa 10132. 81st Annual Meeting of the Meteoritical Society, abstract #6279.
Schenk, P., O'Brien, D. P., Marchi, S., Gaskell, R., Preusker, F., Roatsch, T., Jaumann, R., et al. 2012. The Geologically Recent Giant Impact Basins at Vesta's South Pole. *Science* 336: 694–97.
Schenk, P. M., Neesemann, A., Marchi, S., Otto, K., Hoogenboom, T., O'Brien, D. P., Castillo-Rogez, J., Raymond, C. A., and Russell, C. T. 2022. A Young Age of Formation of Rheasilvia Basin on Vesta from Floor Deformation Patterns and Crater Counts. *Meteoritics & Planetary Science* 57: 22–47.
Schmedemann, N., Kneissl, T., Ivanov, B. A., Michael, G. G., Wagner, R. J., Neukum, G., Ruesch, O., et al. 2014. The Cratering Record, Chronology and Surface Ages of (4)

Vesta in Comparison to Smaller Asteroids and the Ages of HED Meteorites. *Planetary and Space Science* 103: 104–130.

Scott, E. R., and Wasson, J. T. 1976. Chemical Classification of Iron Meteorites—VIII. Groups IC. IIE, IIIF and 97 Other Irons. *Geochimica et Cosmochimica Acta* 40: 103–115.

Scott, E. R., Wasson, J. T., and Buchwald, V. F. 1973. The Chemical Classification of Iron Meteorites—VII. A Reinvestigation of Irons with Ge Concentrations between 25 and 80 ppm. *Geochimica et Cosmochimica Acta* 37: 1957–83.

Scott, E. R. D. 1972. Chemical Fractionation in Iron Meteorites and its Interpretation. *Geochimica et Cosmochimica Acta* 36: 1205–36.

Scott, E. R. D. 2020. Iron Meteorites: Composition, Age, and Origin. In *Oxford Research Encyclopedia of Planetary Science*. Oxford, UK: Oxford University Press.

Scott, E. R. D., Greenwood, R. C., Franchi, I. A., and Sanders, I. S. 2009. Oxygen Isotopic Constraints on the Origin and Parent Bodies of Eucrites, Diogenites, and Howardites. *Geochimica et Cosmochimica Acta* 73: 5835–53.

Spitzer, F., Burkhardt, C., Budde, G., Kruijer, T. S., and Kleine, T. 2020. Isotopic Evolution of the Protoplanetary Disk as Recorded in Mo Isotopes of Iron Meteorites. *51st Lunar and Planetary Science Conference*, abstract #3040.

Spitzer, F., Burkhardt, C., Nimmo, F., and Kleine, T. 2021. Nucleosynthetic Pt Isotope Anomalies and the Hf-W Chronology of Core Formation in Inner and Outer Solar System Planetesimals. *Earth and Planetary Science Letters* 576: 117211.

Spivak-Birndorf, L. J., Bouvier, A., Benedix, G. K., Hammond, S., Brennecka, G. A., Howard, K., Rogers, N., et al. 2015. Geochemistry and Chronology of the Bunburra Rockhole Ungrouped Achondrite. *Meteoritics & Planetary Science* 50: 958–975.

Spurný, P., Bland, P. A., Shrbený, L., Borovička, J., Ceplecha, Z., Singelton, A., Bevan, A. W. R., et al. 2012. The Bunburra Rockhole Meteorite Fall in SW Australia: Fireball Trajectory, Luminosity, Dynamics, Orbit, and Impact Position from Photographic and Photoelectric Records. *Meteoritics & Planetary Science* 47: 163–185.

Srinivasan, G., Goswami, J. N., and Bhandari, N. 1999. ^{26}Al in Eucrite Piplia Kalan: Plausible Heat Source and Formation Chronology. *Science* 284: 1348–50.

Srinivasan, P., Dunlap, D. R., Agee, C. B., Wadhwa, M., Coleff, D., Ziegler, K., Zeigler, R., and McCubbin, F. M. 2018. Silica-Rich Volcanism in the Early Solar System Dated at 4.565 Ga. *Nature Communications* 9: 3036.

Sunshine, J. M., Bus, S. J., McCoy, T. J., Burbine, T. H., Corrigan, C. M., and Binzel, R. P. 2004. High-Calcium Pyroxene as an Indicator of Igneous Differentiation in Asteroids and Meteorites. *Meteoritics & Planetary Science* 39: 1343–57.

Sykes, M. V., and Vilas, F. 2001. Closing in on HED Meteorite Sources. *Earth, Planets and Space* 53: 1077–83.

Tarduno, J. A., Cottrell, R. D., Nimmo, F., Hopkins, J., Voronov, J., Erickson, A., Blackman, E., Scott, E. R. D., and McKinley, R. 2012. Evidence for a Dynamo in the Main Group Pallasite Parent Body. *Science* 338: 939–942.

Thomas, P. C., Binzel, R. P., Gaffey, M. J., Storrs, A. D., Wells, E. N., and Zellner, B. H. 1997. Impact Excavation on Asteroid 4 Vesta: Hubble Space Telescope Results. *Science* 277: 1492–95.

Vaci, Z., Day, J. M. D., Paquet, M., Ziegler, K., Yin, Q.-Z., Dey, S., Miller, A., Agee, C., Bartoschewitz, R., and Pack, A. 2021. Olivine-Rich Achondrites from Vesta and the Missing Mantle Problem. *Nature Communications* 12: 5443.

Wallis, K. F. 2014. Revisiting Francis Galton's Forecasting Competition. *Statistical Science* 29: 420–24.

Warren, P. H. 2011. Stable-Isotopic Anomalies and the Accretionary Assemblage of the Earth and Mars: A Subordinate Role for Carbonaceous Chondrites. *Earth and Planetary Science Letters* 311: 93–100.

Warren, P. H., Rubin, A. E., Isa, J., Brittenham, S., Ahn, I., and Choi, B.-G. 2013. Northwest Africa 6693: A New Type of FeO-Rich, Low-Δ^{17}O, Poikilitic Cumulate Achondrite. *Geochimica et Cosmochimica Acta* 107: 135–154.

Wasson, J., and Kallemeyn, G. 2002. The IAB Iron-Meteorite Complex: A Group, Five Subgroups, Numerous Grouplets, Closely Related, Mainly Formed by Crystal Segregation in Rapidly Cooling Melts. *Geochimica et Cosmochimica Acta* 66: 2445–73.

Wasson, J. T. 1967. The Chemical Classification of Iron Meteorites: I. A Study of Iron Meteorites with Low Concentrations of Gallium and Germanium. *Geochimica et Cosmochimica Acta* 31: 161–180.

Wasson, J. T. 1969. The Chemical Classification of Iron Meteorites—III. Hexahedrites and Other Irons with Germanium Concentrations between 80 and 200 ppm. *Geochimica et Cosmochimica Acta* 33: 859–876.

Wasson, J. T. 1970a. Ni, Ga, Ge and Ir in the Metal of Iron-Meteorites-with-Silicate-Inclusions. *Geochimica et Cosmochimica Acta* 34: 957–964.

Wasson, J. T. 1970b. The Chemical Classification of Iron Meteorites: IV. Irons with Ge Concentrations Greater than 190 ppm and Other Meteorites Associated with Group I. *Icarus* 12: 407–423.

Wasson, J. T. 2013. Vesta and Extensively Melted Asteroids: Why HED Meteorites are Probably not from Vesta. *Earth and Planetary Science Letters* 381: 138–146.

Wasson, J. T. 2017. Formation of Non-Magmatic Iron-Meteorite Group IIE. *Geochimica et Cosmochimica Acta* 197: 396–416.

Wasson, J. T., and Choe, W.-H. 2009. The IIG Iron Meteorites: Probable Formation in the IIAB Core. *Geochimica et Cosmochimica Acta* 73: 4879–90.

Wasson, J. T., and Choi, B.-G. 2003. Main-Group Pallasites: Chemical Composition, Relationship to IIIAB Irons, and Origin. *Geochimica et Cosmochimica Acta* 67: 3079–96.

Wasson, J. T., and Kimbeblin, J. 1967. The Chemical Classification of Iron Meteorites—II. Irons and Pallasites with Germanium Concentrations between 8 and 100 ppm. *Geochimica et Cosmochimica Acta* 31: 2065–93.

Wasson, J. T., Matsunami, Y., and Rubin, A. E. 2006. Silica and Pyroxene in IVA Irons, Possible Formation of the IVA Magma by Impact Melting and Reduction of L-LL-Chondrite Materials Followed by Crystallization and Cooling. *Geochimica et Cosmochimica Acta* 70: 3149–72.

Wasson, J. T., and Schaudy, R. 1971. The Chemical Classification of Iron Meteorites—V Groups IIIC and IIID and Other Irons with Germanium Concentrations between 1 and 25 ppm. *Icarus* 14: 59–70.

Wasson, J. T., and Wang, J. 1986. A Nonmagmatic Origin of Group-IIE Iron Meteorites. *Geochimica et Cosmochimica Acta* 50: 725–732.

Watters, T. R., and Prinz, M. 1979. Aubrites: Their Origin and Relationship to Enstatite Chondrites. *10th Lunar and Planetary Science Conference*, pp. 1073–93.

Wiechert, U. H., Halliday, A. N., Palme, H., and Rumble, D. 2004. Oxygen Isotope Evidence for Rapid Mixing of the HED Meteorite Parent Body. *Earth and Planetary Science Letters* 221: 373–382.

Willis, J., and Goldstein, J. I. 1982. The Effects of C, P, and S on Trace Element Partitioning during Solidification in Fe-Ni Alloys. *Journal of Geophysical Research: Solid Earth* 87: A435–A445.

Wimpenny, J., Sanborn, M. E., Koefoed, P., Cooke, I. R., Stirling, C., Amelin, Y., and Yin, Q.-Z. 2019. Reassessing the Origin and Chronology of the Unique Achondrite Asuka 881394: Implications for Distribution of ^{26}Al in the Early Solar System. *Geochimica et Cosmochimica Acta* 244: 478–501.

Windmill, R. J., Franchi, I. A., Hellmann, J. L., Schneider, J. M., Spitzer, F., Kleine, T., Greenwood, R. C., and Anand, M. 2022. Isotopic Evidence for Pallasite Formation by Impact Mixing of Olivine and Metal During the First 10 Million Years of the Solar System. *PNAS Nexus* 1: pgac015.

Worsham, E. A., Burkhardt, C., Budde, G., Fischer-Gödde, M., Kruijer, T. S., and Kleine, T. 2019. Distinct Evolution of the Carbonaceous and Non-Carbonaceous Reservoirs: Insights from Ru, Mo, and W Isotopes. *Earth and Planetary Science Letters* 521: 103–112.

Xu, S., Binzel, R. P., Burbine, T. H., and Bus, S. J. 1995. Small Main-Belt Asteroid Spectroscopic Survey: Initial Results. *Icarus* 115: 1–35.

Yamaguchi, A., Clayton, R. N., Mayeda, T. K., Mitsuru Ebihara, M., Yasuji Oura, Y., Miura, Y. N., Haramura, H., Misawa, K., Kojima, H., and Nagao, K. 2002. A New Source of Basaltic Meteorites Inferred from Northwest Africa 011. *Science* 296: 334–36.

Yamaguchi, A., Setoyanagi, T., and Ebihara, M. 2006. An Anomalous Eucrite, Dhofar 007, and a Possible Genetic Relationship with Mesosiderites. *Meteoritics & Planetary Science* 41: 863–874.

Yang, J., Goldstein, J. I., Michael, J. R., Kotula, P. G., and Scott, E. R. 2010. Thermal History and Origin of the IVB Iron Meteorites and their Parent Body. *Geochimica et Cosmochimica Acta* 74: 4493–4506.

Yang, J., Goldstein, J. I., and Scott, E. R. 2008. Metallographic Cooling Rates and Origin of IVA Iron Meteorites. *Geochimica et Cosmochimica Acta* 72: 3043–61.

Zhang, B., Chabot, N. L., Rubin, A. E., Humayun, M., Boesenberg, J. S., and van Niekerk, D. 2022. Chemical Study of Group IIIF Iron Meteorites and the Potentially Related Pallasites Zinder and Northwest Africa 1911. *Geochimica et Cosmochimica Acta* 323: 202–219.

Zhang, C., Miao, B., and He, H. 2019. Oxygen Isotopes in HED Meteorites and their Constraints on Parent Asteroids. *Planetary and Space Science* 168: 83–94.

Zhu, K., Moynier, F., Wielandt, D., Larsen, K. K., Barrat, J.-A., and Martin, B. M. 2019. Timing and Origin of the Angrite Parent Body Inferred from Cr Isotopes. *Astrophysical Journal Letters* 877: L13.